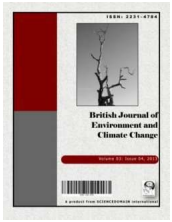

British Journal of Environment & Climate Change
5(3): 231-253, 2015, Article no.BJECC.2015.018
ISSN: 2231–4784

SCIENCEDOMAIN *international*
www.sciencedomain.org

Integrating Weather Research and Forecasting Model, Noah Land Surface Model and Urban Canopy Model for Urban Heat Island Effect Assessment

K. I. Morris[1*], A. Chan[1], S. Aekbal Salleh[2], M. C. G. Ooi[1], Y. A. Abakr[1], M. Y. Oozeer[1] and M. Duda[3]

[1]Faculty of Engineering, University of Nottingham Malaysia Campus, Selangor, Malaysia.
[2]Faculty of Architecture, Planning and Surveying, Universiti Teknologi MARA, Selangor, Malaysia.
[3]National Center for Atmospheric Research NCAR Boulder, CO, USA.

Authors' contributions

This work was carried out in collaboration between all authors. Author KIM designed the study, supervised the model runs and the data analyses and wrote and revised the manuscript. Authors AC and YAA are the academic supervisors of author KIM and provided direction on this research and as well comment on the drafted manuscript. Authors SAS, MCGO, MYO and MD provided suggestions on data used and methods of validation.

Article Information

DOI: 10.9734/BJECC/2015/14923

Original Research Article

Received 28th October 2014
Accepted 20th December 2014
Published 2nd September 2015

ABSTRACT

Despite increased interest on the urban heat island (UHI) phenomenon, there are limited UHI studies on cities built using the green-city concept of Sir Ebenezer Howard [1]. The administrative capital of Malaysia, Putrajaya is one of such cities built using the green-city concept. The objective of this study was to confirm the effectiveness of the green city concept using the National Centre for Atmospheric Research (NCAR) numerical technique. Numerical mesoscale Weather Research and Forecasting (WRF) Model was coupled with Noah land surface model and a single layer urban canopy model (UCM) to investigate the existence and distribution of UHI, and the behavior of urban canopy layer (2-m) temperature of Putrajaya city. Few studies have been conducted using the NCAR numerical technique (WRF) to explore Malaysian climatology. Suitability of the model employed in studying UHI phenomenon of Putrajaya city was determined using in-situ study of the area, and observational data from AlamSekitar Malaysia SdnBhd (ASMA). Contribution of urban fabrics on the spatial and temporal variations of UHI was also investigated. Comparison with ASMA and in-situ data revealed a satisfactory performance of the model.UHI intensity (UHII) of Putrajaya exhibits a diurnal profile; increasing during the night to a peak value and then diminishing towards morning with a negligible value in the mid-day. In the night time, the UHII ranges from

**Corresponding author: Email: kenobimorris@yahoo.com;*

1.9ºC to 3.1ºC in some of the precincts considered. However, the overall effect of the urbanized areas (local climate zones) on the UHI magnitude was normalized by the total amount of area reserved for vegetation.

Keywords: Noah LSM/UCM/WRF; Putrajaya; Urban Heat Island; evaluation.

1. INTRODUCTION

Putrajaya, the administrative capital of Malaysia is a green-concept planned model city. Being first of its kind in the region, it is built to reflect the country's commitment to green environment and to accommodate the growing size of the Malaysian federal government ministries and national level civil servants. The city is structured to accommodate all diplomatic activities, enabling the country to showcase its modernisation agenda [2]. Putrajaya is located in Klang Valley, 25 km south of Kuala Lumpur on coordinates 2°55'00" N 101°40'00" E and covers an approximate area of 49 km^2 (Fig. 1a); which was previously covered by green vegetation, rubber and oil palm plantation before its advent development.

Unlike other cities sprawling from a core with a clear chronology of expansion over decades and in some cases centuries [3-6], the plan of Putrajaya follows the green-city-concept initiated in 1898 by Sir Ebenezer Howard in the United Kingdom [1]. The green-city concept is an idea where cities are planned and builton undeveloped land with a planning garden-city concept [7]. Several cities such as Maringa in Brazil [8], French Dakar city in Senegal [9] and Putrajaya have been built with this concept; most of which are politically envisioned [2]. Despite the lush and colourful canopy afforded to such cities with planned urbanisation, most plans failed to integrate local climate conditions into the garden-city concept leading to consequences such as poor environmental and ecological conditions [7,10,11]. Building cities that are responsive to the local climate conditions and contribute to sustainable environment are some of the challenges facing urban planners.

UHI is a consequence of urbanisation. Urbanisation induces significant changes in the properties of land surface which, in turn, modify the surface energy balance (SEB) of urban areas [12] and hence influencing energy consumption [3,13-16], air quality [17,18], heat related discomfort, mortality [19–23] and local and regional atmospheric circulations [24-26]. UHIs do not have a direct influence on global temperatures [27]; however, they do have impact on local temperatures used to assess climate changes [28,29]. Urban heat island is a common phenomenon in cities notwithstanding the geographical location. The urban-rural temperature difference - urban heat island intensity (UHII) is the most cited measure of climatic modification of a city in environmental sciences [12].

Difference in SEB of urban and rural areas as a consequence of the imbalance in the amount of heat energy stored during the day is the primary cause of UHI development [30]. Earth's Natural vegetation with a near-uniform surface roughness and evapotranspiration properties are being replaced with urban fabrics characterized with high thermal properties; such as asphalts, concretes, bricks and metals [18,31,32]. The surface modifications and enlargement provided by canyon-like geometry and altered thermal properties of natural vegetation enable built up areas to store more radiated heat during the day than do rural areas. Following sunset, urban and rural temperatures begin to diverge thereby generating the heat island in the canopy-layer of the built up areas. Due to the open exposure and unobstructed clear sky view factor of rural area, cooling starts quickly after sunset, this is not the case in built up areas known for slow cooling rate. Slow cooling is attributed to reduced sky view factor and re-radiation of the stored heat energy during the day [31,33]; the heat island stays in the canopy-layer overnight, until sunrise when daily solar radiation cycle begins and rural areas start warming up [34].

Outdoor thermal conditions in urban areas are of major concern in the tropical region of Southeast Asia (SEA). In temperate climate, the maximum UHI effect could be noticed only during the summer season. However, due to the close proximity of the tropical regions to the equator and with high exposure of the region to solar radiation, UHI effect is felt during hot dry season and anytime of the year [35]. Inadequate shading and green spaces are unable to intercept and balance the heat from direct solar gains. Also, conventional use of dark materials in buildings and pavements trap more of the sun's energy

during the day and re-radiate it at night. This has led to air and surface temperature increases with consequent influence on human thermal comfort and building energy consumption in the tropics [22,36,37].

Though, there are few studies in Klang Valley (which encompasses Putrajaya area, Kuala Lumpur and Selangor) on the subject of UHI. Most are *in-situ* studies [38-46] and little or no attention have be given to the subject numerically. Putrajaya, a city with its emergence from an undeveloped palm plantation or almost green vegetation [2] fits to be studied to understand the effectiveness of the "garden-city concept" adopted during its design and planning. Due to non-availability of sufficient data on the area, this study was validated with an hourly surface observational data from AlamSekitar Malaysia SdnBhd (ASMA[1])and corroborated with a recently published *in-situ* study by Ahmed et al., 2014 (investigates the behaviour of surface temperature and heat island effect of Putrajaya main boulevard). Temporal and spatial variation of the UHI of Putrajaya, canopy layer (2-m) air temperature and influence of surface materials were investigated using the advanced core of the NCAR non-hydrostatic meso-scale model, WRF-ARW.

1.1 Weather Research and Forecasting (WRF) Model

The WRF model is a numerical weather prediction (NWP) and atmospheric system designed for research and operational applications [47]. WRF features two dynamical (computational) cores (or *solvers*), a data assimilation system, and a software architecture allowing for parallel computation and system extensibility, and has a non-closure planetary boundary layer (PBL) scheme. The model serves a wide range of meteorological applications across scales ranging from several meters to thousands of kilometres. The model is a collaborative result of National Centre for Atmospheric Research's (NCAR) Mesoscale and Microscale Meteorology (MMM) Division, the National Oceanic and Atmospheric Administration's (NOAA), National Centre for Environmental Prediction (NCEP), Earth System Research Laboratory (ESRL), the Department of Defense's Air Force Weather Agency (AFWA) , Naval Research Laboratory (NRL), the Centre for Analysis and Prediction of Storms (CAPS) at the University of Oklahoma, the Federal Aviation Administration (FAA), and with the participation of other universities around the world.

The WRF single source code could be configured for both research and operational applications. Its spectrums of physics and dynamics schemes available to users reflect the broad scientific community input on the development of the software codes.WRF is maintained and supported as a community model to enable wide use of the software for research, operational and teaching purposes. It is capable of wide range of applications, from large-eddy to global simulations; such as real time numerical weather prediction, physics parameterization research, data assimilation and development studies, air quality simulations, regional climate simulations, urban climatology, atmosphere-ocean coupling and idealized simulations [47].

The principal component of the WRF modelling system includes; WRF software framework (WSF), which provides the infrastructure supporting the dynamics solvers, programs initialization, WRF-Var, WRF-Chem, and physics packages that interface with the solvers. WRF has two dynamic solvers, the Advanced Research WRF (ARW) and the Non-hydrostatic Mesoscale Model (NMM). In this study the ARW is employed.

1.2 Noah Land Surface Model (Noah LSM)

The Noah land surface model is a one-dimensional land surface model describing surface temperature, soil moisture, and soil temperature, snow depth, snow water equivalent, surface energy, water content flux and canopy water content [48,49]. The Noah LSM has seen some improvement over the years. Especially its coverage on snow density, snow depth, maximum snow albedo database and calculation of soil heat flux processes under snow roughness length, snow coverage, and soil thermal conductivity [50,51]. The Noah LSM has a single-canopy layer with four soil layers of varying thicknesses (10, 30, 60 and 100 cm); 10 and 100 cm being the top and bottom layers respectively. This equates the total soil depth of the Noah LSM to 2 m, with the upper and lower 1 m of the soil serving as the root zone depth and reservoir with gravity drainage respectively [34].

[1]*ASMA is a private company who owns 50 Continuous Air Quality Monitoring (CAQM) Stations in Malaysia, one of which is located in Putrajaya*

Different organisations and research institutions have used the Noah LSM in varying applications. For instance, The Noah LSM has been coupled with the Weather Research and Forecasting (WRF) model and other models to investigate phenomena ranging from urban heat island to boundary layer development [51-55]. The operational implementation of the Noah LSM model in the WRF-NMM system at the United States NCEP and in the ARW system at the United States Air Force Weather Agency in 2006 are important milestones in the development of this land surface model.

The newly developed Noah LSM with multiple physics options (Noah-MP) for key land-atmosphere interaction processes provides more representative options [49,56] to parameterize the land surface model. It has been incorporated from WRF version 3.4.1. The Noah- MP LSM integrates dynamic vegetation and groundwater processes, and is more comprehensive in representing the interactions and feedbacks between physical, chemical and biological processes. Most regional weather or climate models in use today do not consider dynamical vegetation and groundwater processes [57]. These processes play an important role in weather and climate simulations, since variations in vegetation, groundwater and soil moisture could last from several weeks to whole seasons [58]. It also contains a separate vegetation canopy designated by a canopy top and bottom, crown radius, and leaves with prescribed dimensions, density, orientation, and radiometric properties. The canopy uses a two-stream radiation transfer scheme along with shading effects required to achieve proper surface energy and water transfer processes including under-canopy snow processes [59,60]. Options are provided for runoff and surface water infiltration, and groundwater transfer and storage including water table depth to an unconfined aquifer.

1.3 Urban Canopy Model (UCM)

The single-layer urban canopy model (SLUCM) is a 2-D street canyons parameterization to represent the effects of urban geometry on urban canyon flux distributions. This was developed by Kusaka et al. [61] to improve representation of urban environment in numerical weather prediction and mesoscale models. The UCM model has undergone some improvement in course of its decade history. The SLUCM considers the urban geometry in its surface energy budget and wind shear computation. The exchange of energy and momentum between the urban surfaces and the atmosphere is handled by the UCM [60]. The canopy model calculates the surface skin temperature of the wall, roof, and the roads as well as heat and momentum fluxes. These parameters are then passed to the WRF model. The UCM also considers shadowing from buildings and reflection of radiations, road orientation and diurnal changes of solar azimuth angle, a multilayer heat equation for wall, roof and road interior temperatures to account for the incoming and outgoing radiation fluxes. Exponential wind profile in the canopy layer, anthropogenic heat release and a thin bucket model for hydrological process are also included in the single-layer urban canopy model [60,62-64].

1.4 Feasibility of Method Employed

While the Noah LSM and SLUCM handles the interactions of surface and canopy layer properties such as soil moisture, heat fluxes, momentum exchange and representation of urban morphology and roughness, the WRF model handles the calculation and iteration of these parameters and as well the provision for inclusion of input data in the form of initial and lower boundary layer conditions. The WRF also accommodates the land use/land cover which provides vital parameters to the coupled model such as surface albedo, soil moisture availability, and surface emissivity, surface heat capacity, snow cover effect, terrain information, soil temperature and surface thermal inertia.

Since Urban heating is induced by variables that span multiple of scales; mesoscale model (2 km-2000 km) [65] would have difficulty to accurately characterise micro-scale (2 mm-2 km) phenomena such as urban heat island [66]. Hence, the SLUCM is incorporated to the WRF model to couple the urban environment and atmospheric conditions; by integrating information such as thermal characteristics and roughness layer of the urban fabric and urban canyon geometry [67]. Thus, the justification of its capability to fairly estimate heating of urban environment.

The coupled model has been used in different regions to study the urban heat island phenomenon, in China [24,54], Singapore [68], and Greece [69]. Due to the success recorded in previous studies of urban heat island using the

coupled WRF/Noah/UCM, same approach of the coupled model has been adopted to investigate the urban heating of Putrajaya City. Verification of the model will be conducted in section 3 of this report.

2. DATA SOURCES

Data from different sources were used in this research study to aid in understanding the climatology of Putrajaya city. Six hourly (1.0° x 1.0°) global Final (FNL) Analysis data were used as the Global Forecast System (GFS) data for Initial and boundary conditions for the simulations. These data were obtained from the National Centre for Environmental Prediction (NCEP)[70]. Hourly surface observational data from AlamSekitar Malaysia SdnBhd (ASMA) and *in-situ* study by Ahmed et al. [7] on investigation of the "urban surface temperature behaviour and heat island effect in a tropical planned city" were used to verify the canopy layer air temperatures (2-m temperature) from the numerical calculations in the study. Google map, Google earth and digitized satellites images were also used for proper depiction and identification of locations, land use (Fig. 1b) and local climate zone (LCZ) classification of the area using [12] guidelines.

2.1 Description of the Study Area

Putrajaya (2°55'00" N 101°40'00" E) is located in the west peninsula of Malaysia and encompassed by the Klang Valley [2]. The city is situated between the Kuala Lumpur International airport on its south axis and the capital city of Malaysia, Kuala Lumpur on its north axis [71] (Fig. 1a). In line with the Putrajaya's master plan, the development of the city which started in 1993 is due to be completed by the year 2025 [7]. The master plan is characterized by the "garden-city" concept which integrates physical features such as landforms, vegetation and water bodies which form the green scenery of the city. To reflect the country's pledge to adhere to environmental standards, about 38% of the total land area of Putrajaya is reserved for wetlands, green space and water bodies [72]. Though, the developments of the main boulevard and its surrounding precincts is near completion, only about 60 percent of the intended master plan has been completed to date [7]. Despite the delay in completion of the master plan, Putrajaya is a host to an approximate 100,000 residents of the projected 350,000 residents when completed [2].

With few degrees off north of the equator and with an average elevation of 30 m (Fig. 1c) [2], Putrajaya sits on a hilly terrain with a humid and hot weather all year. Rainfall averages 2-3 m in a year and falls heavily during the monsoon season, depositing about 10 to 30 cm within few hours [73]. Proximity to the equator exposes the area to high solar radiation accounting to about 6.1 hours of sunshine per day all year round; hence the hot and humid climate experienced with a near steady average air temperature (27.5ºC and 25ºC, maximum and minimum respectively), 62.6% humidity and wind speed ranging from 0 - 7.5 m/s [74]. The artificial lakes and wetlands delineate Putrajaya into core and peripheral areas. One of the mainland marks of the Putrajaya concept design is the main Boulevard (Fig. 2d). The main boulevard measures 100 m wide, and extends 4.2 km from the northeast to the southwest of Putrajaya and cuts along five core precincts of the area (1, 2, 3, 4 and 5) (Fig. 2d) [74]. Surrounded by government symmetric buildings oriented northwest to southeast, the main boulevard separates the administrative area with the surrounding streets. The urban form of Putrajaya area could simply be described as a characteristic fusion of different local climate zones (LCZs[2]) as described in Stewart & Oke" local climate zone classifications for urban temperature studies"[12].

Like Chandigarh in India, Putrajaya is divided into 21 precincts with each of the precincts dedicated to distinct functions ranging from commerce, entertainment, housing, foreign diplomats and government. Unlike the Chandigarh's system of identical 'sectors', Putrajaya's precincts have been built visually distinct from one another through clustering buildings.

2.2 *In-situ* Data of Putrajaya

In an attempt to investigate the urban heat island of the city, Ahmed et al. [7] conducted an *in-situ* measurement of surface temperature, ground temperature (LST) and wind velocity on a clear sky and cloudless day from 14 – 16th July, 2012 along the main boulevard covering precincts 1, 2, 3 and 4. Surface temperature and wind velocity were measured for 3 days from 14 to 16th July, 2012 along the main boulevard.

[2]*local climate zone (LCZ) as region of uniform surface cover, structure, material, and human activity that span hundreds of meters to several kilometres in horizontals scale [12].*

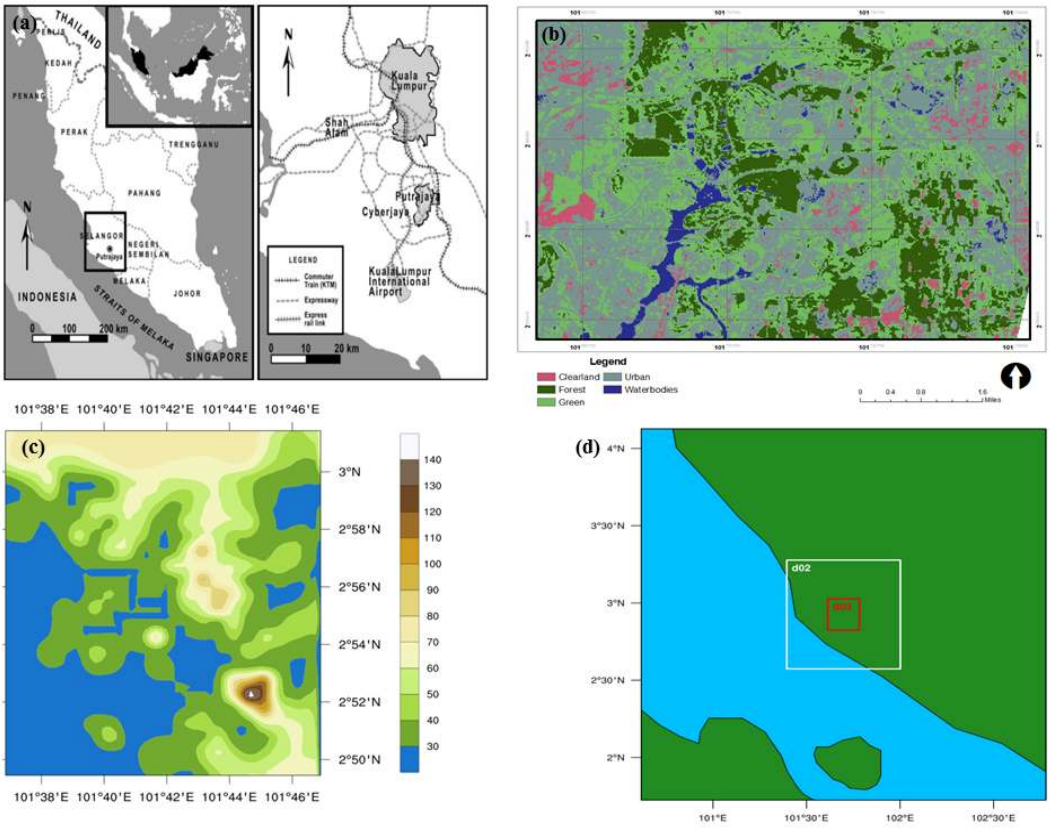

Fig. 1. (a) Putrajaya location (source: Moser, 2010). (b) Putrajaya 2012 Land use. (c) Terrain height (m) of the inner nested domain (relative to mean sea level). (d) Configuration of the 3 one-way nested domains for WRF simulation

Air temperatures were measured at two different characteristics locations at different times for 13 and 18th July for one location and 20 and 28th July, 2012 for the other. Locations with different land cover types were also used in their investigation. Fluke 63 infrared thermometer at a height of 1.65 m and Data logger TR-72U at a height of 3 m were used to measure surface and air temperatures respectively [7].

2.3 Hourly Meteorological Observational Data from ASMA

ASMA is a private company in Malaysia saddled with maintenance and collation of hourly meteorological data using about 52-networks of Continuous Automatic and Manual Air Quality Monitoring (CAQM) stations in Malaysia. These stations were built between 1995 and 2000 [75]. Meteorological data among which are air temperature, wind speed, humidity and ozone are out source by the Malaysian department of environment (DOE) and are made available to environment-related authorities and research groups. CAQMs are often used as the primary data sources for climatic research. They provide input for statistical analyses and can further be utilised for the formation of models or frameworks. Depending on the research objectives, data from these instruments can be used to validate findings, study atmospheric, weather and meteorological conditions at a specific window of time in the location where experiment took place. This is important to synthesize and rationalize the research findings relationship with actual conditions. Historical data from these instruments allow climate researchers to study the backdated environmental conditions and help to recognise the patterns and trends for future predictions.

CAQM comprises of measurement instrumentation (for both pollutant gases and meteorological parameters); support instrumentation (support gases, calibration equipment); instrument shelters (temperature

controlled enclosures); and data acquisition systems (to collect and store data). Also, the fitted sensor for measuring air temperature is at an altitude of approximately 3 m above ground level (a.g.l) (Fig. 2a, b & c).

CAC053 (02º55'54.9N 101º40'54.5E) is the designated ID of the only CAQMS station situated in Putrajaya. This station is fitted with sensor to measure air temperature at an altitude 3 m (a.g.l). CAC053is located in precinct 8 on an open field with nearby classrooms and has a source area characterized by open low-rise LCZ built (Fig. 2c).

3. METHODOLOGY AND EVALUATION

Using guidelines provided in [12,76,77] for metadata collections and source area (represented by physical surface properties as obtained in Table 1 of [78]) delineation; Source areas were set to encompass a 100 m radius from sites of data collections in dense urban surroundings (e.g. city core) and 200 m radius for more open fetch areas (e.g. city outskirts). This is necessitated by varying magnitude of advection within dense and open fetch areas and thus the impact on the transport of re-radiated fluxes during calmed nights. Horizontal spatial classification of LCZ zone were adopted from the definition of 0.1 km – 10 km ([78,79], p. 3,4). Hence, the definitions of immediate land cover types and LCZ used in characterizing different sites in this study (Table 1).

3.1 Numerical Configuration

To study the temperature distribution and UHI of the nascent Putrajaya city, 13th to 28th July 2012 were simulated with interest on the canopy-layer (2-m) air temperature. These days were selected to coincide with the dates studied by [7] to establish the basis for comparison and validation of the model.

Table 1. Characteristics of data extraction sites during the study

Name	Latitude (° N)	Longitude (° E)	Altitude (m.a.s.l[3])	Built type (LCZ)	Immediate land cover of sites source area
P3	2°54'57.06"	101°41'2.40"	32	Open midrise	Pave su rface
P4	2°54'27.72"	101°40'44.40"	38	Sparsely built	Low plants & paved surface
P6	2°53'58.85"	101°39'57.60"	25	Sparsely built	Bare rock/soil
P7	2°55'45.88"	101°40'26.40"	42	Open midrise	Paved surface
P8	2°56'5.10"	101°40'55.20"	42	Compact low-rise	Paved surface
P9	2°56'24.86"	101°40'33.60"	39	Open midrise	Paved surface
P10	2°56'44.09"	101°41'13.20"	32	Open low-rise	Pave d surface
P12	2°57'23.08"	101°42'21.60"	49	Compact low-rise	Bare soil & dense trees
P13	2°57'52.16"	101°41'42.00"	35	Sparsely built	Bar e soil & dense trees
P17	2°55'16.79"	101°42'10.80"	43	Open midrise	Scatt ered trees
P20	2°53'0.64"	101°40'44.40"	14	Sparsely built	Low plants
BLV1[4]	2°55'26.40"	101°41'13.20"	29	Sparsely built	Paved surface
BLV2	2°54'47.45"	101°41'2.40"	37	Sparsely built	Pa ved surface
IR[5]	2°57'52.16"	101°42'43.20"	49	Sparsely built	Low pl ants
TMP[6]	2°55'45.88"	101°42'3.60"	47	Open low-rise	Paved su rface & scattered trees
Ahmed_P4	2°55'6.67"	101°41'4.12"	39	Open midrise	Pa ved surface
Ahmed_P3	2°55'36.03"	101°41'13.90"	31	Open midrise	Paved surface
CAC053	2°55'54.9"	101°40'54.5"	33	Open low-rise	Ope n field & paved surface
Rural	2°49'46.30"	101°37'49.67"	11	Open low-rise	Ba re soil & Scattered trees

[3] *Above sea level*
[4] *Putrajaya main Boulevard*
[5] *IOI Resort ➔ Palm Garden Gulf Club*
[6] *Taman Warisan Pertanian*

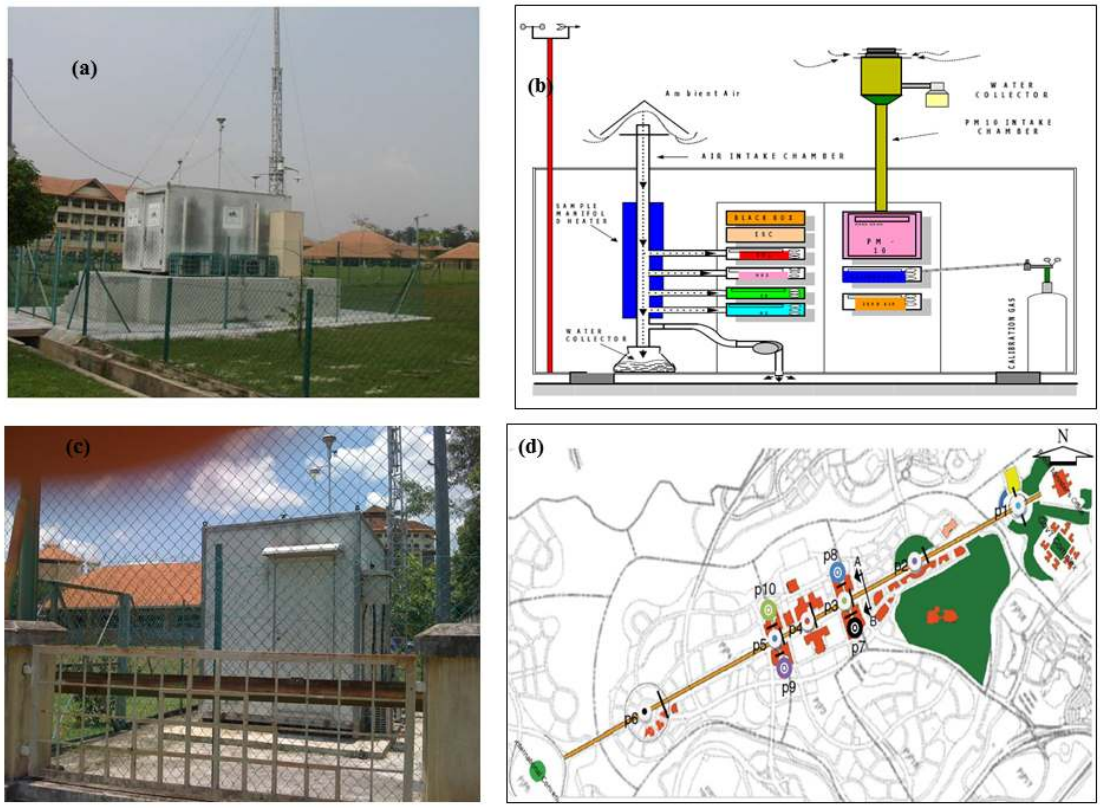

Fig. 2. (a) Automatic Air Quality Monitoring Station. (b) CAMQs schematic diagram (source: DOE, 2008). (c) Putrajaya CAQMs. (d) Cross-section showing Putrajaya main boulevard and intersecting precinct (source: Ahmed et al., 2014)

Version 3.5 of the WRF-ARW (Advanced Research Weather) model was used as the meteorological model for numerical calculations.; WRF-ARW is a numerical weather prediction and atmospheric simulation system which integrates the advanced core of the WRF model dynamics solver [47]. This system combines the Unified Noah land-surface model (LSM) [48], coupled with the single-layer urban canopy model (UCM).

The planetary boundary layer (PBL) was handled with the Yonsei University (YSU) scheme [80], combined with the coupled Noah/UCM land surface model; as it is considered to perform well in studying urban climates in high resolution applications [80,52]. Other physics parameterisations include a long wave Rapid Radiative Transfer Model (RRTM) [81], a short-wave radiation scheme based on Dudhia cloud radiation scheme [82] and a surface-layer scheme based on the MM5Monin-Obukhov similarity theory. The WRF single-moment six-class (WSM-6) microphysics scheme was applied to all domains [83,84], while parameterization of cumulus convection was completed using Kain-Fritsch scheme [85]. However, the snow option for the WSM-6 microphysics was disabled since the area is not known for snowing.

Three one-way nested domain (Fig. 1d) with horizontal grid spatial resolutions of 2.7, 0.9 and 0.3 km which contained 90 × 100, 76 × 88 and 64 × 76 grid boxes respectively, from west to east and south to north for parent (d01), 1st nested (d02) and innermost (d03) domain respectively. WRF uses terrain-following hydrostatic-pressure vertical coordinate system proposed by [86] to resolve the vertical layers of the model. In this study, 32 vertical levels were used, 18 of which were reserved in the lower 2 km of the model to better resolve the lower atmosphere while the model top layer was specified at 100 hPa.; this is to accommodate the frequent changes of atmospheric variables in the lower boundary layer and as well as to handle the small scale features near the Earth's surface. However, the coarse vertical spacing of the

sigma higher levels is to reduce computational cost [87].

Updated high resolution MODIS data land use and land cover (LULC) classification of the International Geosphere-Biosphere Programme and modified Noah land surface model were used for the land use and land cover aspects of the study; with 2-arc-min, 30-arc-sec, and 30-arc-sec spatial resolution used for d01, d02 and d03 respectively. This data is modified and updated regularly by the National Centre for Environmental Predictions (NCEP) to be used for the WRF/Noah LSM model. The need to understand phenomena such as urban heat island in microclimates has made the need for high resolution LULC classification more imperative. The regularly updated dataset are freely available and could be obtained at the same download site as the WRF source codes (www2.mmm.ucar.edu/wrf/users/download/get_source.html).

The Noah land surface model (LSM) was employed to parameterize the land surface processes [48]. The updated Noah LSM is a land surface-hydrology model [34] and serves to provide surface sensible and latent heat fluxes, account for sub-grid fluxes and as well skin temperature as lower boundary conditions to the boundary layer scheme of the WRF. Noah LSM uses conduction, diffusion tracer and viscous transport of momentum mechanism to complete transport of surface sensible and latent heat fluxes between the surface and lowest millimetre of air diffusion [50,63].

The single-layer UCM has a unique simplified two-dimensional urban geometry model, considering building height, roof and road width and assuming street canyons of infinite length. It also includes solar trapping and reflection of radiation and shadowing effects, which is determined by the street canyon dimensions and orientation, as well as the solar azimuth angle. Thus, the energy and momentum transfer between an urban environment and the atmosphere could be calculated by computing surface temperatures and heat fluxes of roof, wall and road within the considered area. Coupling the WRF model with Noah LSM completes the urban surface energy balance (SEB), by calculating fluxes from vegetated portion of urban surface in a given grid cell. In this study the UCM model was modified to reflect the prevailing urban morphological and surface conditions of Putrajaya via the urban parameter table (URBPARM.TBL) using information derived from [7,12,74,88]. Though, the single-layer urban canopy model (UCM) coupled with the WRF model is considered an effective tool in predicting urban heat island of urban areas [89], it is yet to be validated in tropical region of Malaysia. This study used both *in-situ* and meteorological observation to corroborate the performance of the WRF coupled to the Noah LSM and UCM.

3.2 Model Initialization

$1^{o}\times 1^{o}$ spatial resolution and 6 h temporal resolution operational global atmospheric final re-analysis (FNL) surface and pressure level data of the NCEP were used for initialization of the model simulation. This product is from the Global Data Assimilation System (GDAS), which collates observational data from the Global Telecommunications System (GTS) and other sources for the various analyses (rda.ucar.edu/datasets/ds083.2/). Same model used by NCEP in the Global Forecast System (GFS) is also adopted for the NCEP FNL. In the surface boundary layer and at some sigma layers (tropopause), the data are available on the surface at 26-mandatory and other pressure levels starting from 1000 mbars to 10 mbars. Parent domain (d01) lateral boundary conditions were linearly interpolated from the NCEP FNL 6-hourly data used, while Lateral boundary conditions for d02 and d03 were supplied via interpolated data from the parent domain. The 4-layers (10, 30, 60 and 100 cm) of the Noah LSM temperature and soil moisture values were also initialized from the NCEP-FNL data. Communication through the nested and parent domains is by 1-way process since a one-way feedback activated between is applied to the model via the input name list.

In this study, model run was set to 12:00 UTC of 12^{th} July, 2012 (corresponding to 20:00 MST[7] of 12^{th} July, 2012) for a total run period of 390 h.

3.3 Model Evaluation

Series of simulations were conducted with the WRF model and different physics, microphysics and cumulus options utilized to obtain set of options which streamline the model error to acceptable range before proceeding with model set-up for the duration of study.

[7] *MST – Malaysian Standard Local Time*

Air temperature is an important parameter in urban climatology and has been used in several published studies to validate different model performances [34,90-92]. To establish a common basis for comparison of model and observed results, model results were obtained at same locations and corresponding time as observations results.

It is unlikely to determine the performance of any model without the application of statistical tools. Four statistical tools were employed in this study to evaluate the performance of the model (WRF) used for the predicted results (*P*) and observed results (*O*); both for ASMA and *in-situ* (P3 and P4) [7]. In this study P3 and P4 designate Figs. 14 and 15o f Ahmed et al. [7] investigation respectively. More details about locations P3 and P4 as used in Ahmed et al. [7] are given in results and discussion section of this paper. Mean bias error (MBE), mean absolute error (MAE), root mean square error (RMSE) and Pearson correlation coefficient (R) were used to access the model performance and agreement with the observed data. The square of the Pearson coefficient (R^2), also known as the coefficient of determination measures the strength and direction of linear relationship between *P* and *O,* R^2also tells the degree of variance between *P* and *O* as described by the linear fit ([93], pp. 258–67). MBE measures the inclination of the model to over predict or under predict an event. It does not provide insight on the magnitude of the typical error; therefore, it is not used as an indicator for accuracy. However, the MAE is an accuracy measurement and could easily be thought of as the typical magnitude of the predicted error [93]. Like the MAE, RMSE estimates the expected magnitude of error associated with a model's prediction [94]. The RMSE is used in comparison and evaluation of simulation models to measure the model accuracy and precision [95]. For good correlation between *P* and *O* data, the R^2 should range from 0.5 – 1.0 [93], with coefficient of determination of 1.0 indicating good correlation between the predicted and observed variables and R^2 of 0 indicating no correlation.

Comparison of the WRF simulated results and observed values in each case indicated good correlation between *P* and *O* (Figs. 3a, b and 4). The model overestimated the canopy layer air temperature for ASMA station CAC053, although, the MAE magnitude was within acceptable range. The model performed relatively well when compared with *in-situ* observation by Ahmed et al. 2014[7] (Fig. 4).

4. RESULTS AND DISCUSSION

4.1 Canopy-Layer Air Temperature

The amount of intensity of solar radiation reaching a given location on the earth's surface depends on the azimuth angle sunlight strikes the earth's ground surface. The azimuth angle at a particular location decreases from high to low during sunrise to sunset. Effect of the diurnal behaviour of the azimuth angle coupled with the surface albedo induces temporal warming of the location. Fig. 5 presents a 24 hours modelled 2-m temperatures averaged over data extraction sites (Table 1) for the duration of study (13/07/2012 to 28/07/2012). The temperature profile of the city during the study period exhibits same diurnal profile as observed in other cities [96-98]. An averaged minimum temperature of 24.5ºC and maximum temperature of 31.2ºC were observed at 0800 and 1600 MST.

Fig. 6 shows the modelled canopy-layer (C-L) air temperatures for 13th of July, 2012at different period characterized by temporal and spatial heating of the urban canopy. The model was able to capture the spatial and temporal variation of C-L air temperatures. Modelled spatial variation of C-L air temperature is due to the differential heating of different LCZs in the study area and this agrees with [12]. The LCZs (Table 1) are marked with different built and land cover types exhibiting different surface albedos resulting from the composition of the surface materials. Temporal CL-air temperatures are driven by the diurnal cycle of sunrise and sunset.

4.2 Canopy-Layer UHI

Urban canopy-layer extends vertically from the ground level up to the mean roof level of any given local urban climate zone. The urban-rural and LCZs (LCZ-LCZ) temperature contrast observed within this layer is referred to as the canopy layer UHI [30]. As recommended by [34,99], caution was observed in the selections process of the sites to eliminate the unwanted effects that surface relief, elevation and other surface variability would impact on the magnitude of the UHI. Nineteen (19) different sites with similar topographic features (Table 1) were selected for this study. Eighteen (18) of which

are within Putrajaya; representing different LCZs and One (1) representing the rural/semi-urban conditions is located outside of Putrajaya. As such, induced influence of surrounding local climates due to advection and transport were minimized by locating the rural station in an area isolated from other urban influences. Also, to ensure that UHII are correctly interpreted, 40 m (Table 1) maximum elevation difference between sites was used as criterion for sites selection [34].

4.2.1 Canopy-layer UHI – rural-urban

Malaysia is known for differential precipitation between local climates; therefore, days with similar favourable synoptic conditions for UHI study(such as calm days with low surface wind speed and weak horizontal pressure gradient resulting in clear skies and devoid of precipitation) were considered to investigate the rural-urban canopy layer UHI experience in Putrajaya during the study period. The absent of a meteorological station in the rural site in this study poseda setback; however, precipitation records obtained on (www.weathercity.com) were used instead. Precipitation data for Putrajaya were obtained from the Malaysian meteorological department (MMD)[100]. 13th, 15th, 18th, 23th and 26th of July, 2012 were considered for the rural-urban heat island investigation. The rural site (Fig. 7b) designated "Rural" is situated about 4 km southwest of Putrajaya at an elevation of 11 m above mean sea level (Table 1). Its LCZ is characterized by open low-rise built type with a bare soil and scatter trees source area as land cover (Table 1 and Fig. 7b).

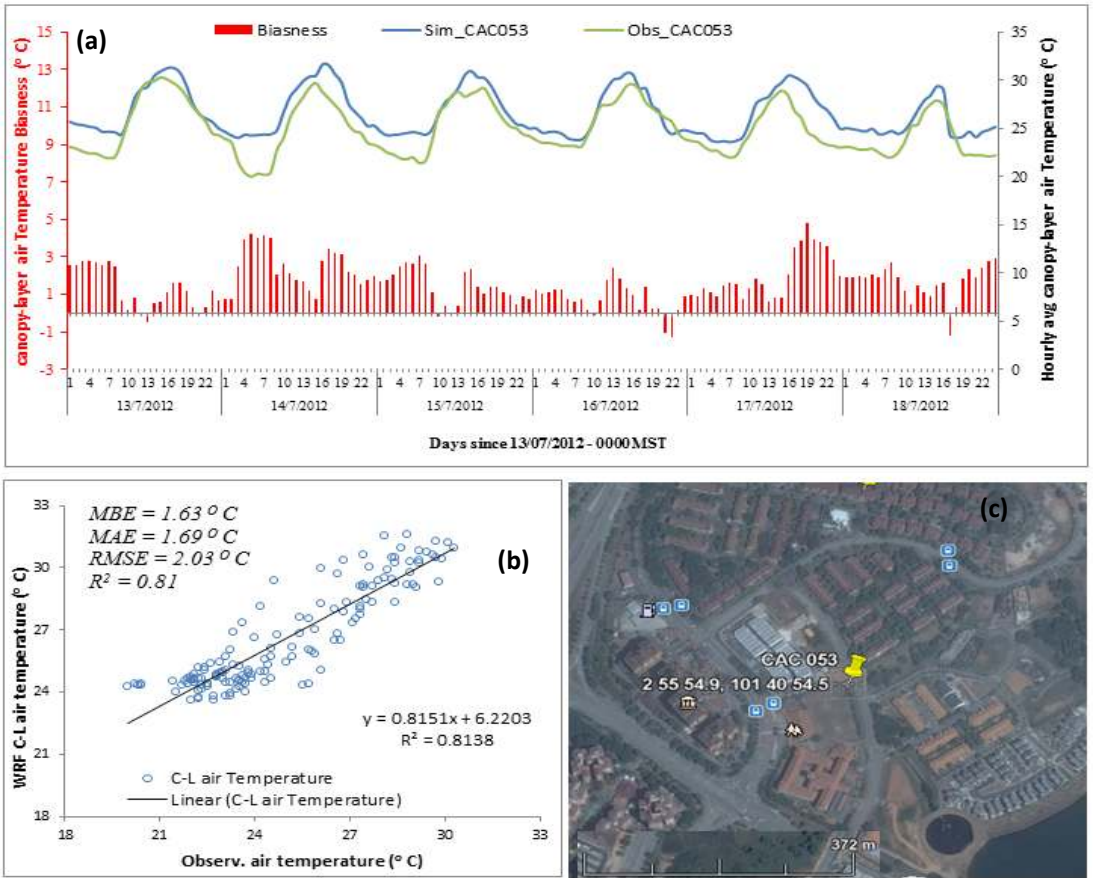

Fig. 3. (a) Model validation at Putrajaya ASMA station CAC053, (b) scatter plot for canopy layer air temperatures of CAC053, (c) location of ASMA station (source: Google-Earth). The blue line indicates model results and green line for observed and red line for the biasness between the model and observed results. Refer to Table 1 for characteristics of P3 & P4

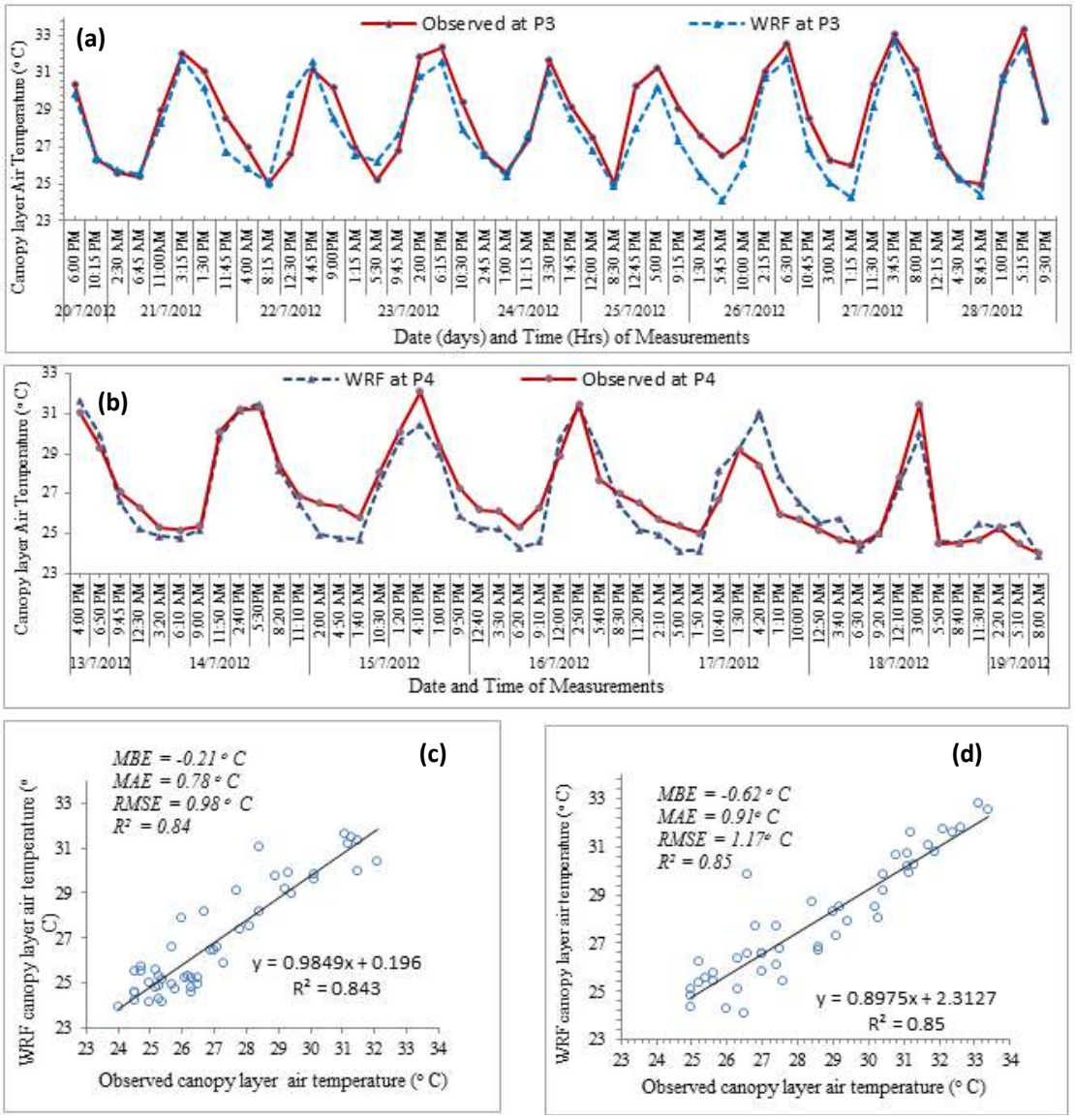

Fig. 4. (a) and (b) Model validation for location P3 and P4 respectively (source: Ahmed et al., 2014, Figs. 14 & 15 respectively), (c) and (d) are scatter plots for canopy layer air temperatures for location P3 and P4 respectively. Blue lines indicate model results, while red lines indicate observed results.

Fig. 8 shows averaged heating of the area for the selected days with a profile representing the diurnal behaviour of UHI as exhibited in different studies in other cities [34,52,101]. Timing of sunrise and sunset (roughly 0700 and 1900 MST respectively) seem to have induced influence on the magnitude of the UHII experienced in the area. During mid-day, intensity of solar energy reaches the surface of the earth uniformly. Despite the differential absorption of heat fluxes in engineered surfaces that characterized the urbanized Putrajaya and the semi-natural surfaces of the rural site during this period, heating in both areas is overshadowed by the constant and uniform amount of sunlight striking the surface of the earth. Thus, negligible urban canopy-layer heating was noticed during mid-hours (1100 – 1700 MST) of the considered days. However, an urban heat sink was observed from 1300 – 1600 MST.

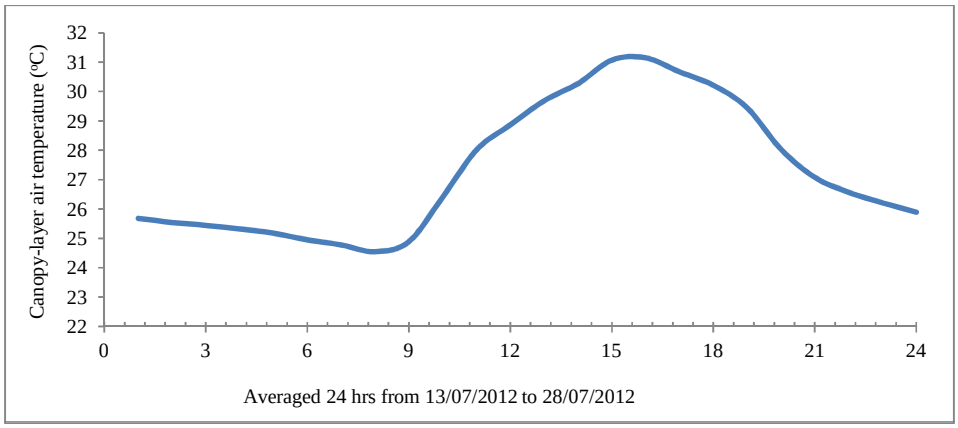

Fig. 5. 24 hours averaged modelled canopy-layer air temperature (ºC) for the study period - 13/07/2012 to 28/07/2012

4.2.2 Canopy-layer UHI – LCZ-LCZ

The term urban heat island is often associated with rural-urban temperature contrast; however, within an urban area, a temperature difference could be noticed between different local climate zones. This is as a result of the varying factors (such as land cover type, building height, aspect ratio, etc.) that differentiate LCZs. Such difference in urban canopy layer air temperature is induced by varying land cover and built types (Figs. 7 and 9). The magnitude of LCZ – LCZ UHI is driven temporally by solar radiation variations. To evaluate the LCZ-LCZ UHI in the area, LCZs with varying built and land cover source area types were selected. Precinct 8 (Fig. 7e), 3, (Fig. 7f) and 20 (Fig. 7d),characterized by compact low-rise and pave surface, open midrise and pave surface, and sparsely built and low plants respectively (Table 1) were compared with precinct 13 (sparsely built and low plants). 13th of July, 2012 was selected to study the UHI phenomenon in the LCZs. Figs. 6 and 9 presents the behaviour of the LCL-LCZ UHI and the dependency of its magnitude on built and source area land cover type. Open midrise had the highest magnitude with a negligible heating observed for precinct 20.

4.3 Impact of Surface Materials on the Intensity of UHI

Putrajaya is composed of different LCZs with varying land surface materials. For instance, P3, P7, P9, P10, P12 and others as contained in Table 1 are marked with paved surfaces as the source area, while the remaining sites are marked with a combination of low plants, trees and bare soil or paved surfaces. These materials have different thermal properties and thus different rate of heat absorption and retention. Fig. 9 portrays the impact of surface materials on the magnitude of the UHI. Though the number of sites used in this study is too small to generalize on UHI impacts, it is an indication of a possible contribution and would be further investigated in subsequent studies.

4.4 Discussion

The performance of the WRF-model was assessed with data obtained from ASMA meteorological station and two other *in-situ* measurement sites conducted by (Ahmed et al. 2014). Fig. 3a presents the observed and modelled canopy-layer air temperatures for the ASMA site designated CAC053. Overall, the model performed relatively well for this site and have replicated the phase of diurnal cycle with a correlation coefficient of R^2 of 0.81 and a MAE of 1.69ºC, and RSME of 2.03ºC (Fig. 3b). However, the model overestimated the amplitude of the observed data, especially the night-time minimum temperature. This could imply that either the upward heat fluxes or the outgoing long wave radiation of the area is overestimated and or, radiation of solar trapping and fluxes from walls and roads, producing high ambient temperatures, inside the urban street as calculated in the UCM may have resulted in this discrepancy as the station is few meters (6 – 10) radius away from buildings; hence it is less thermally loaded. The actual causes of the overestimation of temperatures can only be speculated at this stage but could not be concluded due to lack of comprehensive measurements of surface energy balance parameters of the area during the considered period.

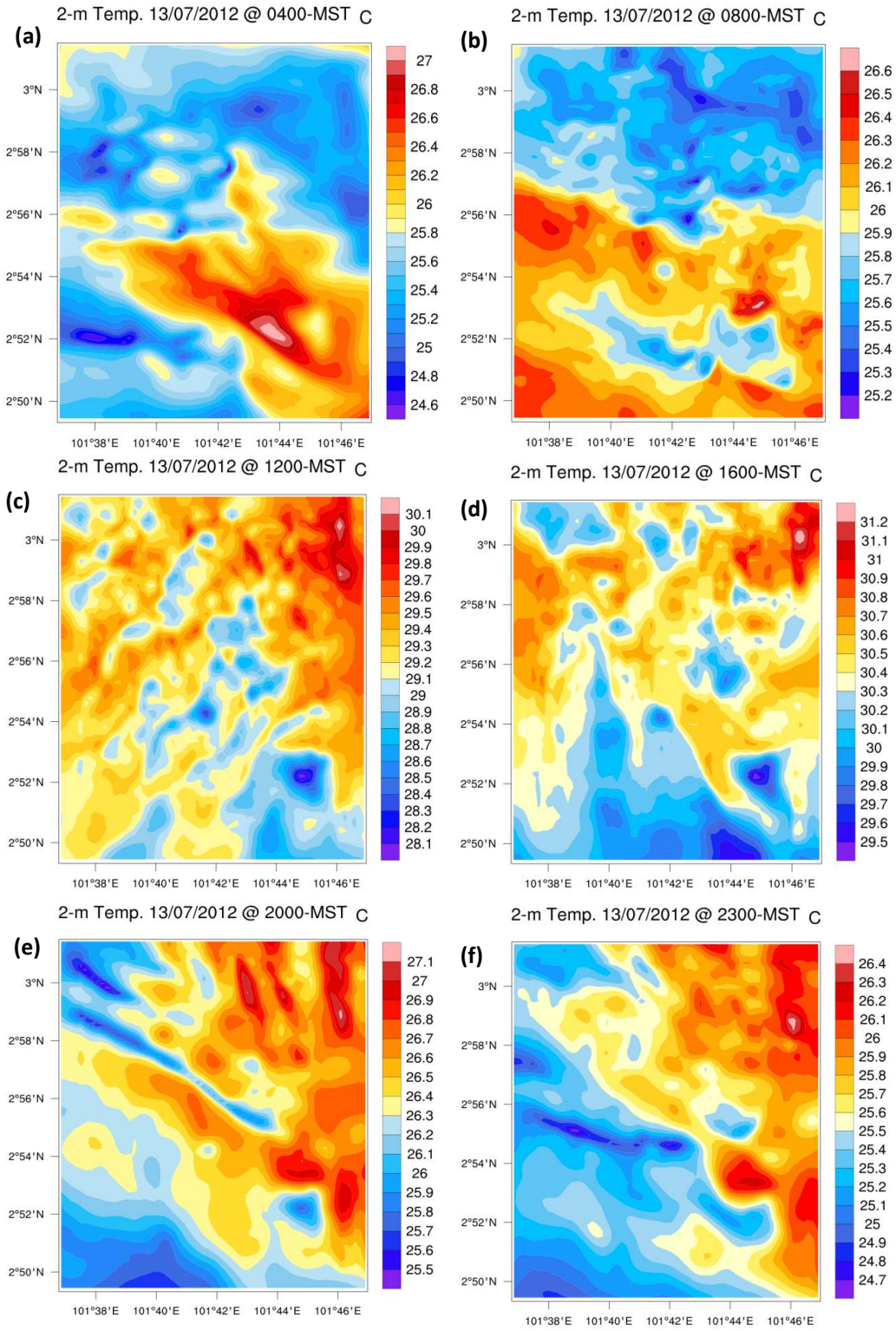

Fig. 6. Modelled spatial and temporal distribution of canopy-layer (2-m) air temperature for 13/07/2012. (a) early morning at 0400 MST, (b) morning at 0800 MST, (c) noon at 1200 MST, (d) daytime at 1600 MST, (e) night at 2000 MST and (f) late night at 2300 MST

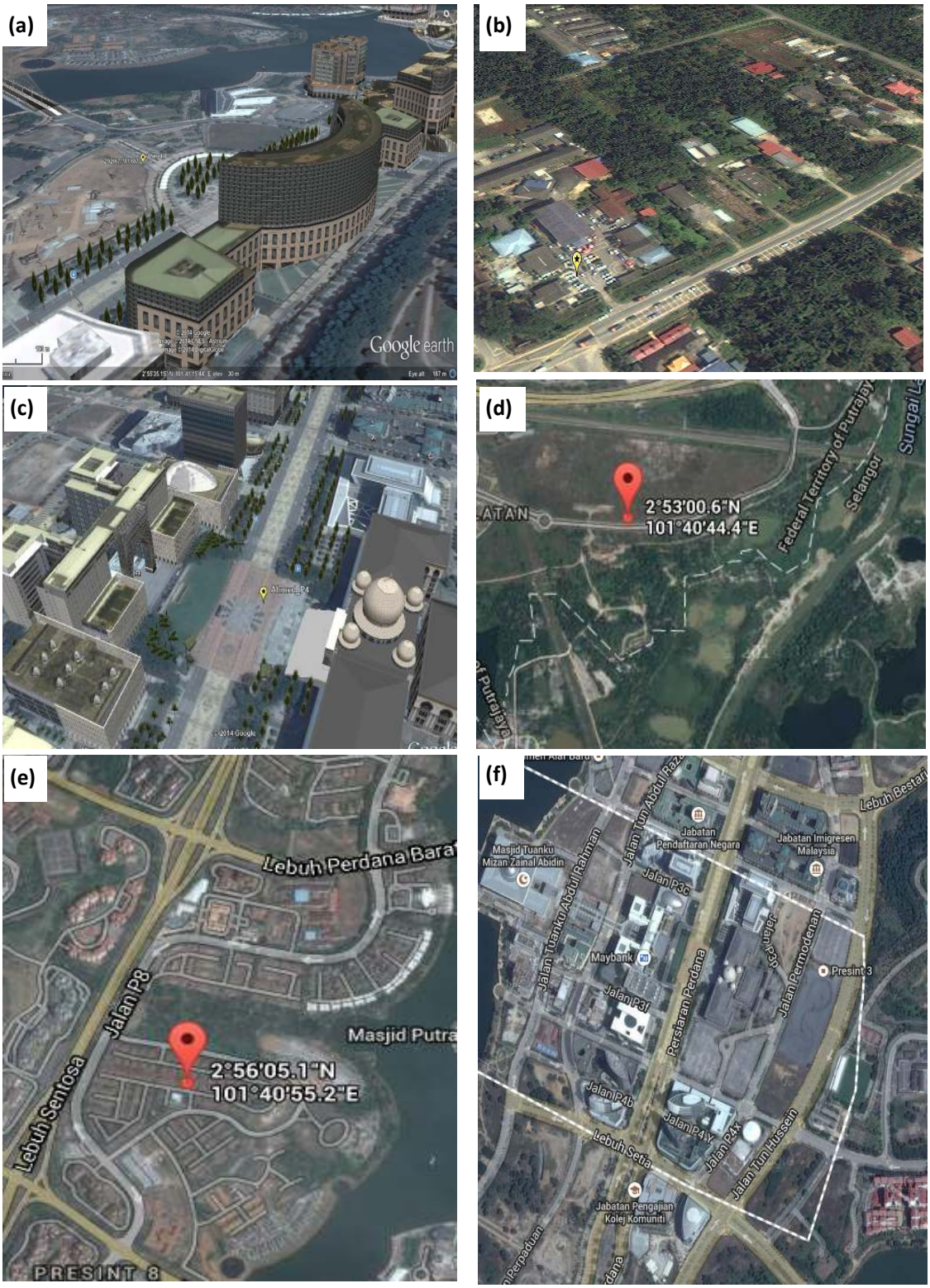

Fig. 6. Google-Earth and Google-map images of the considered areas for this study (a) site for P3, (b) Rural site for UHI study, (c) site for P4, (d) Precinct 13, (e) Precinct 8 and (f) Precinct 3

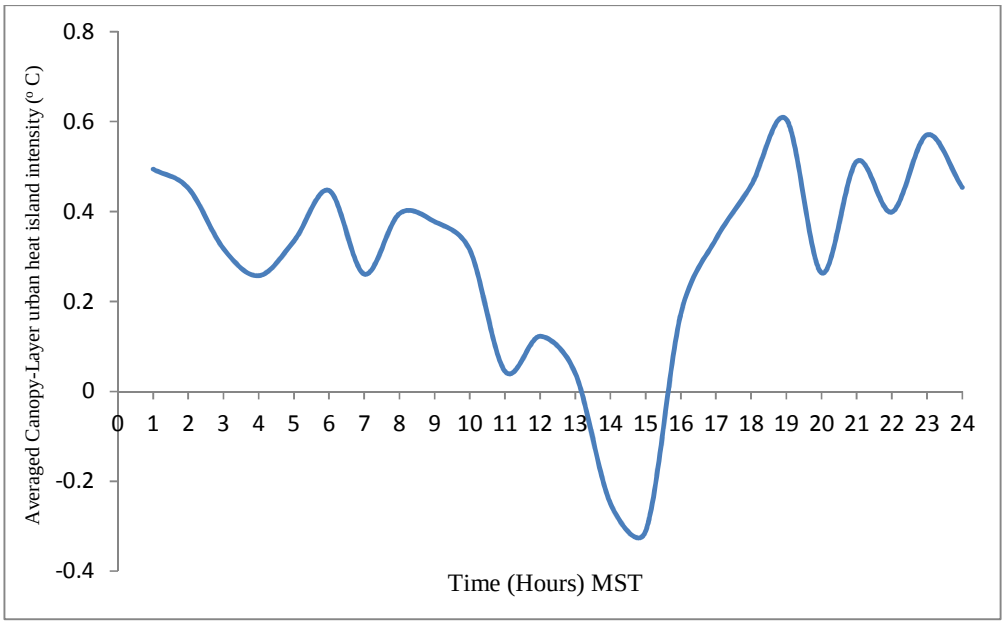

Fig. 7. Averaged canopy layer UHII for the duration of study selected days

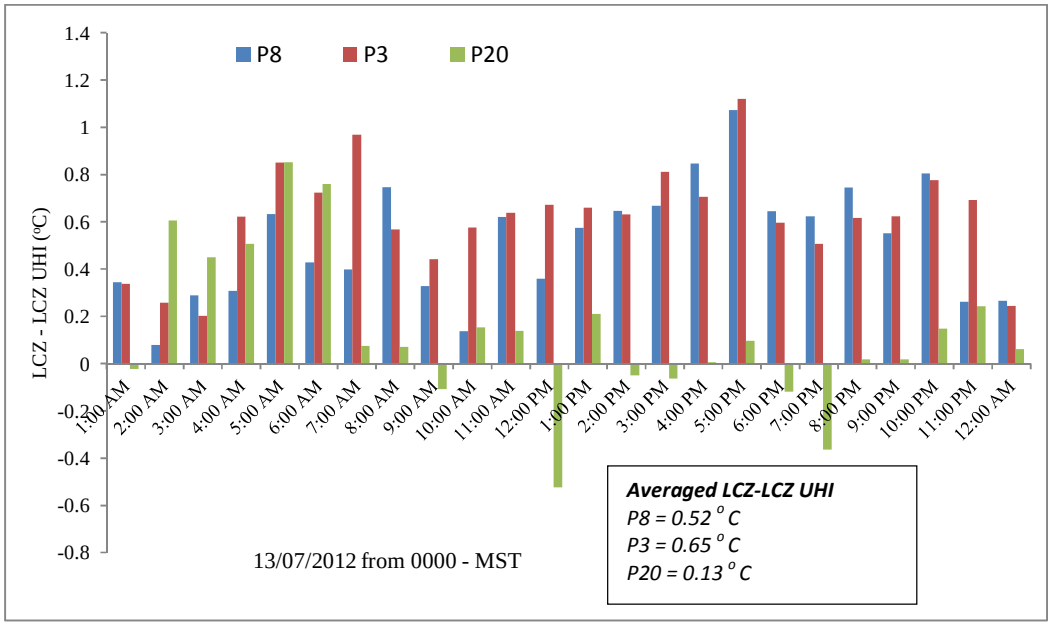

Fig. 8. LCZ - LCZ in Putrajaya for 13/07/2012. Blue, red and green colour bars representing precinct 8, 3 and 20 respectively

Figs. 4a and 4b compared the model (WRF) performance with a recently published case study by [7] in a section of the studied area (Putrajaya Main Boulevard). Statistical analysis shows that the model has performed fairly well with R^2 values of 0.84, 0.85 and RMSE values of 0.98 and 1.17ºC for sites *P3* and *P4* (Fig. 4) respectively. In each of the compared sites (*P3* and *P4*) the model underestimated the phase amplitudes of [7] with MBE of -0.21 and -0.62ºC respectively (Figs. 4c and 4d). The biases probably have resulted from the parameterization of the model using the average properties of the city. However, the considered area is

characterized with low surface albedo materials such as asphalt, concrete and dark-coloured materials in its road and building constructions. Also, the limited amount of vegetation compared to other parts of Putrajaya could have induced this temperature contrast (see Figs. 7a and 7c).

Twenty four hours average 2-m temperature during the study period (13/07/2012 to 28/07/2012) reveals a common trend of diurnal profile of temperature with a minimum and maximum value of 24.5ºC and 31.2ºC respectively. The temperature increases during the day and decreases at night with the minimum and maximum temperatures occurring at 0700 and 1600 MST respectively. This is due to the variation in the amount of solar radiation exposure during the night and day time. The welcome of sunrise (0700 MST) in the area gradually increases the C-L air temperature from 0800 MST. This increase is due to increasing amount of solar energy reaching the earth's surface. Similarly, after sunset (1900 MST), the amount of solar energy reduces and hence the decrease in the C-L air temperature (Fig. 5).

A graphical representation of the modelled UHII of the rural-urban canopy layer is shown in Fig. 8 for a 5-day average overa24 hour time interval. The UHI was computed by subtracting the C-L air temperature of the rural LCZ site from the spatially averaged urban LCZ sites (Table 1). The urban heat island effect is more obvious during the night (1700 – 2300 MST) than the day, and start diminishing in the early morning (0100 – 0600 MST). However, a heat sink was noticed during the hours of 1300 to 1500 MST. Heat sink is the event of a reverse phenomenon of the UHI (i.e. rural areas having higher temperature contrast than the urban). The urban heat sink formation during the day is encouraged by the accumulative effect of the 37% total land area of Putrajaya reserved for vegetation (Fig. 1b). Similarly the reserved vegetation has helped in normalizing the overall impact of the urbanized LCZs on the urban heat island of the area despite some areas such as precinct 3, 7, 8 and 9 having a maximum UHII ranging from 1.9 to 3.1ºC during the study period. Furthermore, the increase in the UHII during the night is due to the slower nocturnal cooling of the urban LCZs resulting from the engineered surfaces used in buildings and constructions of roads. Horizontal transport would be more pronounced in the rural site due to the prevailing LCZ built type (sparsely built); meaning fewer obstructions to impede advection of the re-radiated heat fluxes in the rural site as opposed to the urban climate zones. A maximum UHII of 3.1ºC was observed in Precinct 8 on the 23rd of July, 2012. However, due to the normalizing effects induced by some of the LCZs within the study area with large amount of vegetation, a maximum averaged UHII over the eighteen (18) sites during the selected days was noted to be 0.61ºC.

Much effort on the study of urban heat island effect have been channelled to understanding the temperature contrast between rural and urban areas, little have been done to understand the temperature discrepancy between LCZs. In an attempt to explore this temperature contrast between LCZs; three different LCZs each with distinct built type and source area land cover type were selected for this investigation (Fig. 9) on 13th of July, 2012. Fig. 9 presents the temporal observations of the UHII. Precinct 3characterised of open midrise built type and paved surfaces as source area land cover has the averaged maximum UHII with a magnitude of 0.65ºC followed by precinct 8 (Fig. 9 and Table 1), while precinct 20 has a negligible magnitude of UHII. Precinct 20 has the same characteristics of built type and source area land cover type. This agrees with [102] on the impact of land cover and surface properties as the real drivers of local climate difference.

Spatial and temporal patterns of the UHII were observed in Fig. 6 for 13th of July, 2012. Fig. 6 shows the modelled Graphical representation of the C-L (2-m) air temperatures in the early morning (0400 MST), morning (0800 MST), and noon (1200 MST), during the solar peak time (1600 MST), evening (2000 MST) and late evening (2300 MST). Magnitude of UHI effect is more pronounced during early morning and night time (>1.5ºC), while a negligible effect was observed in day time, indicated by near-uniform contour spread (Figs. 6e and 6f)). The near-uniform contour contrast starts disappearing as evening approaches (indicating increase in UHII) to a clear distinction in the contours spread, indicating a spatial variations in temperatures. This agrees with the stated theory of urban heat island formation by Oke [30].

Fig. 9 highlights the impact of surface materials on the magnitude of UHI. Precinct 8 and 3 are characterized with prevailing paved surfaces and similar built type properties. Conversely, precinct 13 and 20 are predominantly dense trees and low plants respectively. To further understand the induced influence of surface materials on the

area, the average hourly C-L air temperature of precinct 13 for 13/07/2012 was computed and subtracted from the other precincts (3, 8 and 20). Results showed that precincts 3 and 8 have significant UHII than 20. This is due to the differences in the albedo of the surfaces(see Table 4 of Stewart & Oke 2012, p.1887). Greenery is known for their ability to cool the surrounding by evapotranspiration [18,31]. This may have induced the low temperature values experienced in precinct 20 and the average temperature of Putrajaya city.

UHI of the city in this study could not be compared with that obtained by [7] since the current study considered the overall effect on the city as opposed to [7], who concentrated on the Putrajaya main boulevard. Comparatively, with UHI studies conducted in Kuala Lumpur [7,46,103,104], the UHII observed in Putrajaya is relatively lower and this could be accounted for by the 37% of the total land area reserved for vegetation and the yet to be developed areas (Fig. 1b). Therefore, it is evident that the garden city concept adopted for the design and development of Putrajaya city has impact on the magnitude of UHI observed.

5. CONCLUSION

Although the canopy layer surface temperature of Putrajaya is lower compared to cities in other regions, it is pertinent to highlight the need to reduce the temperature of the area during solar peak period. In this paper, the characteristics of the UHI and impact of the garden-city concept adopted during the development of the area were investigated using the single-layer urban canopy model coupled with the WRF/Noah LSM modelling system. Meteorological data from ASMA and *in-situ* data from (Ahmed et al. [7]) were used for the validations of the model, with correlation coefficient ranging from 0.81 to 0.85.

Comparison of model results with the data used for validations showed reasonable correlation and performance. The model reasonably reproduced the phase cycle and diurnal behaviour of the validated data and successfully simulated some of the features of UHI effect such as day and night variations in magnitude. Thus, the model displayed suitability for use in the study of UHI phenomenon, spatial and temporal variations of temperature in the area and as well indicating the general adequacy of using the single-layer UCM in WRF.

Based on high resolution of the simulation and capability of the coupled model employed, we observed that UHI intensity of Putrajaya varies temporally and spatially, with a maximum magnitude of 3.1ºC observed on 23rd July, 2012. However, a maximum average of 0.61ºC UHII over the study period was observed. This is due to the effectiveness of the green city concept in reducing the average urban heating to the bare minimum.

A preliminary comparison of different LCZs showed influences of land cover types on the magnitude of UHI. LCZs characterised with more percentage of vegetation were found to exhibit lower UHII. Furthermore, the reserved total land area for vegetation in Putrajaya may have induced positive influence on the magnitude of urban heat island intensity of the city; with UHII during the night ranging from 1.9 to 3.1ºC. Spatial and temporal variation of C-L air temperature and UHII were also noticed with peak variation during night time. In addition, Intra-urban (LCZ-LCZ) UHI of the study area was also successfully investigated.

The study concludes that the area is heating less compared to other cities (such as Hong Kong with UHII of 10.5ºC [105] and Singapore with 4ºC [106]; nevertheless, there is still need to further reduce the C-L air temperature of the area to achieve the modern green-city plan and the country's pledge of adhering to environmental standards. These preliminary findings would help in optimizing the WRF model and as well facilitate more improvement on the numerical measurement of air temperature and UHI phenomenon in the area.

ACKNOWLEDGEMENTS

This current study is conducted with support through the e-Science fund of the Ministry of Science, Technology and Innovation (MOSTI) with contract number M0056.54.01. The authors would also like to thank Adeb Qaid Ahmed for supplying the data used for the validation of the numerical model employed in this study.

COMPETING INTERESTS

Authors have declared that no competing interests exist.

REFERENCES

1. Howard E. Garden cities of to-morrow, in an introductory essay by Lewis Mumford, Osborn FJ, Ed. London: Faber and Faber. 1946;50–57,138–147.
2. Moser S. Putrajaya: Malaysia's new federal administrative capital. Cities. 2010;27(4):285-297.
3. Martilli A. An idealized study of city structure, urban climate, energy consumption and air quality. Urban Clim. 2014;1-17.
4. Zeng C, Liu Y, Stein A, Jiao L. Characterization and spatial modeling of urban sprawl in the Wuhan Metropolitan Area, China. Int. J. Appl. Earth Obs. Geo-Inf. 2015;34:10–24.
5. Alsharif AAA, Pradhan B. Urban sprawl analysis of Tripoli metropolitan city (Libya) using remote sensing data and multivariate logistic regression model. J. Indian Soc. Remote Sens. 2013;42(1):149-163.
6. Inostroza L, Baur R, Csaplovics E. Urban sprawl and fragmentation in Latin America: A dynamic quantification and characterization of spatial patterns. J. Environ. Manage. 2013;115:87-97.
7. Ahmed AQ, Ossen DR, Jamei E, Manaf NA, Said I, Ahmad MH. Urban surface temperature behaviour and heat island effect in a tropical planned city. Theor. Appl. Climatol; 2014.
8. Macedo J. Maringá: A British garden city in the tropics. Cities. 2011;28(4):347-359.
9. Bigon L. Garden City' in the tropics? French Dakar in comparative perspective. J. Hist. Geogr. 2012;38(1):35-44.
10. Johnson C. Green modernism: The irony of the modern garden cities in Southeast Asia. 44th ISOCARP Congress. 2008;1-11.
11. Xin LZ, Bo L, Li ZL. Water Resource's ecological counteraccusation towards garden city. Procedia Environ. Sci. 2011;10(no. ESIAT):2518-2524.
12. Stewart ID, Oke TR. Local climate zones for urban temperature studies. Bull. Am. Meteorol. Soc. 2012;93(12):1879-1900.
13. Konopacki S, Akbari H. Energy savings for heat-island reduction strategies in Chicago and Houston (including updates for Baton Rouge, Sacramento and Salt Lake City), Berkeley; 2002.
14. Kolokotroni M, Giannitsaris I, Watkins R. The effect of the London urban heat island on building summer cooling demand and night ventilation strategies. Sol. Energy. 2006;80(4):383-392.
15. Akbari H. Energy saving potentials and air quality benefits of urban heat Island mitigation. First International Conference on Passive and Low Energy Cooling for the Built Environment. 2005;1-19.
16. Hirano Y, Fujita T. Evaluation of the impact of the urban heat island on residential and commercial energy consumption in Tokyo. Energy. 2012;37(1):371-383.
17. Wang T, Jiang F, Deng J, Shen Y, Fu Q, Wang Q, Fu Y, Xu J, Zhang D. Urban air quality and regional haze weather forecast for Yangtze River Delta region. Atmos. Environ. 2012;58(2):70-83.
18. Rosenfeld AH, Akbari H, Romm JJ, Pomerantz M. Cool communities: Strategies for heat island mitigation and smog reduction. Energy Build. 1998;28(1): 51-62.
19. Uejio CK, Wilhelmi OV, Golden JS, Mills DM, Gulino SP, Samenow JP. Intra-urban societal vulnerability to extreme heat: The role of heat exposure and the built environment, socioeconomics and neighborhood stability. Health Place. 2011;17(2):498-507.
20. Ihara T, Kusaka H, Hara M, Matsuhashi R, Yoshida Y. Estimation of mild health disorder caused by urban air temperature increase with midpoint-type impact assessment methodology. J. Environ. Eng. 2011;76:459-467.
21. Fire and Disaster Management Agency of Japan. Fire and Disaster Management Agency of Japan; 2011.
22. Enete IC, Officha M, Ogbonna CE. Urban heat Island magnitude and discomfort in Enugu urban area, Nigeria. J. Environ. Earth Sci. 2012;2(7):77-83.
23. Md Din MF, Lee YY, Ponraj M, Ossen DR, Iwao K, Chelliapan S. Thermal comfort of various building layouts with a proposed discomfort index range for tropical climate. J. Therm. Biol. 2014;41:6-15.
24. Miao S, Chen F, LeMone MA, Tewari M, Li Q, Wang Y. An observational and modeling study of characteristics of urban heat Island and boundary layer structures in Beijing. J. Appl. Meteorol. Climatol. 2009;48(3):484-501.
25. Marrapu P. Local and regional interactions between air quality and climate in New Delhi: A sector based analysis. University of Iowa; 2012.

26. Feng JM, Wang YL, Ma ZG, Liu YH. Simulating the regional impacts of urbanization and anthropogenic heat release on climate across China. J. Clim. 2012;25(20):7187-7203.
27. IPCC. Climate change 2001: The scientific basis. Cambridge University Press, Cambridge, United Kingdom and New York, NY, USA; 2001.
28. Van Weverberg K, De Ridder K, Van Rompaey A. Modeling the contribution of the Brussels heat Island to a long temperature time series. J. Appl. Meteorol. Climatol. 2008;47(4):976-990.
29. Barker T. Climate change 2007: An assessment of the intergovernmental panel on climate change. IPCC, Valencia, Spain; 2007.
30. Oke TR. The energetic basis of the urban heat island. Q. J. R. Meteorol. Soc. 1982;108(455):1-24.
31. Taha H. Urban climates and heat islands: Albedo, evapotranspiration and anthropogenic heat. Energy Build. 1997;25(2):99-103.
32. Yang X. Temporal variation of urban surface and air temperature, University of Hong Kong; 2013.
33. Offerle B, Grimmond CSB, Fortuniak K. Heat storage and anthropogenic heat flux in relation to the energy balance of a central European city centre, Int. J. Climatol. 2005;25(10):1405–1419.
34. Giannaros TM, Melas D, Daglis IA, Keramitsoglou I, Kourtidis K. Numerical study of the urban heat island over Athens (Greece) with the WRF model, Atmos. Environ. 2013;73(0):103–111.
35. Tran H, Uchihama D, Ochi S, Yasuoka Y. Assessment with satellite data of the urban heat island effects in Asian mega cities, Int. J. Appl. Earth Obs. Geoinf. 2006;8(1):34–48.
36. Wijeyesekera DC, Affida N, Binti R, Nazari M, Lim SM, Idrus M, Masirin M, Walsh J. Investigation into the urban heat island effects from asphalt pavements, OIDA Int. J. Sustain. Dev. 2012;5(6):97–118.
37. Shaharuddin A, Noorazuan A, Yaakob M, Noraziah M. Accelerated Urbanisation and the Changing Trend of Rainfall in Tropical Urban Areas, World Appl. Sci. J. 2011;13:69–73.
38. Elsayed I. Effects of Urbanization on the Urban Heat Island of Kuala Lumpur City. Saarbrucken, Germany: Lap lambert Academic Publishing. 2012;1–364.
39. Ahmad S, Hashim N, Jani YM. Fenomena Pulau Haba Bandar dan isu alam sekitar di Bandaraya Kuala Lumpur The Urban Heat Island phenomenon and the environmental issues of Kuala Lumpur City, Malaysian J. Soc. Sp. 2009;5(3):57–67.
40. Sani S. Urban Development And Changing Patierns of Night Time Temperatures In The Kuala Lumpur-Petaling Jaya Area Malaysia, J. Teknol. 1984;5(1).
41. Ilham SM. Elsayed. A study on the urban heat island of the city of kuala lumpur, malaysia, in 19th Conference on Applied Climatology. 2011;1–6.
42. Yusof M, Johari M. Identifying green spaces in kuala lumpur using, Alam Cipta. 2012;5(2):93–106.
43. Elsayed ISM. Mitigation of the Urban Heat Island of the City of Kuala Lumpur, Malaysia, Middle-East J. Sci. Res. 2012;11(11):1602–1613.
44. Yusuf YA, Pradhan B, Idrees MO. Spatio-temporal Assessment of Urban Heat Island Effects in Kuala Lumpur Metropolitan City Using Landsat Images, J. Indian Soc. Remote Sens; 2014.
45. Ibrahim I, Samah AA. Preliminary study of urban heat island: Measurement of ambient temperature and relative humidity in relation to landcover in Kuala Lumpur, in 2011 19th International Conference on Geoinformatics. 2011;1–5.
46. Ahmad S, Hashim N, Jani YM, Aiyub K, Mahmod MF. The effects of different land uses on the temperature distribution in urban areas, in SEAGA 2010-Online Proceedings. 2010;1–18.
47. Skamarock WC, Klemp JB, Dudhia J, Gill DO, Barker DM, Duda MG, Huang XY, Wang W, Powers JG. A Description of the Advanced Research WRF version 3. NCAR Technical Note. Boulder, Colorado, USA: National Center for Atmospheric Research: Mesoscale and Microscale Meteorology Division. 2008;1–113.
48. Chen F, Dudhia J. Coupling an Advanced Land Surface–Hydrology Model with the Penn State–NCAR MM5 Modeling System. Part I: Model Implementation and Sensitivity, Mon. Weather Rev. 2001; 129(4):569–585.
49. Niu GY, Yang ZL, Mitchell KE, Chen F, Ek MB, Barlage M, Kumar A, Manning K, Niyogi D, Rosero E, Tewari M, Xia Y. The community Noah land surface model with multi parameterization options (Noah-MP): 1. Model description and evaluation with

local-scale measurements, J. Geophys. Res. 2011;116(D12):D12109.
50. Barlage M, Chen F, Tewari M, Ikeda K, Gochis D, Dudhia J, Rasmussen R, Livneh B, Ek M, Mitchell K. Noah land surface model modifications to improve snowpack prediction in the Colorado Rocky Mountains, J. Geophys. Res. 2010; 115(D22):D22101.
51. Li D, Bou-Zeid E, Barlage M, Chen F, Smith JA. Development and evaluation of a mosaic approach in the WRF-Noah framework, J. Geophys. Res. 2013;118(21):11918–11935.
52. Lin CY, Chen F, Huang JC, Chen WC, Liou YA, Chen WN, Liu SC. Urban heat island effect and its impact on boundary layer development and land–sea circulation over northern Taiwan. Atmos. Environ. 2008;42(22):5635–5649.
53. Xu L. What Do We Learn from Coupling a Next Generation Land Surface Model to a Mesoscale Atmospheric Model?. University of California, Davis; 2012.
54. Miao S, Chen F. Enhanced modeling of latent heat flux from urban surfaces in the Noah/single-layer urban canopy coupled model. Sci. China Earth Sci; 2014.
55. Kusaka H, Kimura F, Coupling a Single-Layer Urban Canopy Model with a Simple Atmospheric Model: Impact on Urban Heat Island Simulation for an Idealized Case. J. Meteorol. Soc. Japan. 2004;82(1):67–80.
56. Yang ZL, Niu GY, Mitchell KE, Chen F, Ek MB, Barlage M, Longuevergne L, Manning K, Niyogi D, Tewari M, Xia Y, The community Noah land surface model with multiparameterization options (Noah-MP): 2. Evaluation over global river basins. J. Geophys. Res. 2011;116(D12):D12110.
57. Zu-heng HU, Zhong-feng XU, Ning-Fang Z, Zhu-Guo M, Guo-Ping L. Evaluation of the WRF Model with Different Land Surface Schemes: A Drought Event Simulation in Southwest China during 2009-10. Atmos. Ocean. Sci. Lett. 2014;7(2):168–173.
58. Schlosser CA, Milly PCD. A Model-Based Investigation of Soil Moisture Predictability and Associated Climate Predictability. J. Hydrometeorol. 2002;3(4):483–501.
59. Niu GY, Yang ZL. Effects of vegetation canopy processes on snow surface energy and mass balances. J. Geophys. Res. 2004;109(D23):D23111.
60. Kusaka H, Kondo H, Kikegawa Y, Kimura F. A simple single-layer urban canopy model for atmospheric models: Comparison with multi layer and slab models. Boundary Layer Meteorol. 2001;101(3):329–358.
61. Ryu YH, Baik JJ, Lee SH. A New Single-Layer Urban Canopy Model for Use in Mesoscale Atmospheric Models. J. Appl. Meteorol. Climatol. 2011;(50)9:1773-1794.
62. Kusaka H, Kimura F. Thermal Effects of Urban Canyon Structure on the Nocturnal Heat Island: Numerical Experiment Using a Mesoscale Model Coupled with an Urban Canopy Model. J. Appl. Meteorol. 2004;43(12):1899–1910.
63. Tewari M, Chen F, Kusaka H, Miao S. Coupled WRF / Unified Noah / Urban-Canopy Modeling System 1 What is an Urban Canopy Model (UCM). Boulder CO, Japan; 2007.
64. Ikeda R, Kusaka H. Proposing the Simplification of the Multilayer Urban Canopy Model: Intercomparison Study of Four Models, J. Appl. Meteorol. Climatol. 2010;49(5):902–919.
65. Oke TR. Boundary Layer Climates, 2nd ed. Routledge. 1988;1–464.
66. Mirzaei PA, Haghighat F. Approaches to study Urban Heat Island – Abilities and limitations. Build. Environ. 2010;45(10): 2192–2201.
67. Chen F, Kusaka H, Bornstein R, Ching J, Grimmond CSB, Grossman-Clarke S, Loridan, Manning KW, Martilli A, Miao ST, Sailor D, Salamanca FP, Taha H, Tewari M, Wang X, Wyszogrodzki Aa, Zhang C. The integrated WRF/urban modelling system: development, evaluation, and applications to urban environmental problems. Int. J. Climatol. 2011;31(2):273–288.
68. Li XX, Koh TY, Entekhabi D, Roth M, Panda J, Norford LK. A multi-resolution ensemble study of a tropical urban environment and its interactions with the background regional atmosphere. J. Geophys. Res. Atmos. 2013;118(17): 9804–9818.
69. Papangelis G, Tombrou M, Dandou A, Kontos T. An urban 'green planning' approach utilizing the Weather Research and Forecasting (WRF) modeling system. A case study of Athens, Greece. Landsc. Urban Plan. 2012;105(1–2):174–183.
70. NCEP. National Centers for Environmental Prediction/National Weather Service/ NOAA/U.S. Department of Commerce. 2000, updated daily. NCEP FNL

Operational Model Global Tropospheric Analyses, continuing from July 1999, 2000. [Online]. Available:http://dx.doi.org/10.5065/D6M043C6. [Accessed: 14-Sep-2013]

71. Mulligan K, Elliott SJ, Schuster-Wallace C. The place of health and the health of place: dengue fever and urban governance in Putrajaya, Malaysia. Health Place. 2012;18(3):613–20.
72. Chin HS. Putrajaya – Administrative Centre of Malaysia -Planning Concept and Implementation. in Sustainable urban development and Governance conference at SungKyunKwan University Seoul. 2006;1–20.
73. Bunnell T. Multimedia Utopia? A Geographical Critique of High-Tech Development in Malaysia's Multimedia Super Corridor. Antipode. 2002;34(2):265–295.
74. Shahidan MF, Jones PJ, Gwilliam J, Salleh E. An evaluation of outdoor and building environment cooling achieved through combination modification of trees with ground materials. Build. Environ. 2012;58:245–257.
75. Awang MB, Jaafar B, Abdullah M, Ismail MB, Hassan MN, Abdullah R, Johan S, Noor H. Air quality in Malaysia: impacts, management issues and future challenges. Respirology. 2000;5(2):183–96.
76. Aguilar E, Auer I, Brunet M, Peterson TC, Wieringa J. Guidelines on climate metadata and homogenization. WMO Tech Doc. Geneva: World Meteorological Organization. 2003;1186:1–53.
77. Oke TR. Initial guidance to obtain representative meteorological observations at urban sites. IOM Rep. 81, WMO. Tech. Doc. No. 1250. World Meteorological Organization, Geneva; 2004.
78. Stewart ID, Oke TR, Krayenhoff ES. Evaluation of the 'local climate zone' scheme using temperature observations and model simulations. Int. J. Climatol. 2014;34(4):1062–1080.
79. Oke TR. Street design and urban canopy layer climate. Energy Build. 1988;11(1–3):103–113.
80. Hong SY, Noh Y, Dudhia J. A New Vertical Diffusion Package with an Explicit Treatment of. Mon. Weather Rev. 2006;134(9):2318–2341.
81. Mlawer EJ, Taubman J, Brown PD, Iacono MJ, Clough SA. Radiative transfer for inhomogeneous atmospheres: RRTM, a validated correlatedk model for the longwave. J. Geophys. Res. 1997; 102(D14):16663–16682.
82. Dudhia J. Numerical Study of Convection Observed during the Winter Monsoon Experiment Using a Mesoscale Two-Dimensional Model J. Atmos. Sci. 1989;46(20):3077–3107.
83. Hong SY, Dudhia Ji, Chen SH. A Revised Approach to Ice Microphysical Processes for the Bulk Parameterization of Clouds and Precipitation. Mon. Weather Rev. 2004;132 (1):103–120.
84. Dudhia J, Hong SY, Lim KS. A New Method for Representing Mixed-phase Particle Fall Speeds in Bulk Microphysics Parameterizations. J. Meteorol. Soc. Japan. 2008;86A:33–44.
85. Kain JS. The Kain–Fritsch Convective Parameterization: An Update J. Appl. Meteorol. 2004;41(1):170–181.
86. Laprise R. The Euler Equations of Motion with Hydrostatic Pressure as an Independent Variable. Mon. Weather Rev., 1992;120(1):197–207.
87. Chou S. An Example of Vertical Resolution Impact on WRF-Var Analysis. Electron. J. Oper. Meteorol. no. May, 2011;EJ05.
88. Aekbal S, Abd Z, Mohd W, Wan N. Social and Factors Contributing to the Formation of an Urban Heat Island in Putrajaya, Malaysia. Procedia - Soc. Behav. Sci. 2013;UE–004:1–11.
89. Subramania Pillai S, Yoshie R. Experimental and numerical studies on convective heat transfer from various urban canopy configurations J. Wind Eng. Ind. Aerodyn. 2012;104–106:447–454.
90. Mercader J, Codina B, Sairouni A, Cunillera J. Results of the meteorological model WRF-ARW over Catalonia, using different parameterizations of convection and cloud microphysics. Tethys, J. Weather Clim. West. Mediterr. 2010;75–86.
91. Hu Z, Yu B, Chen Z, Li T, Liu M. Numerical investigation on the urban heat island in an entire city with an urban porous media model. Atmos. Environ. 2012;47:509–518.
92. Shem W, Shepherd M. On the impact of urbanization on summertime thunderstorms in Atlanta: Two numerical model case studies. Atmos. Res. 2009;92(2):172–189.
93. Wilks DS. Statistical methods in the atmospheric sciences, 2nd Editio. Oxford,

UK: International Geophysics Series. 2006;1–627.
94. Lundy CC, Brown RL, Adams EE, Birkeland KW, Lehning M. A statistical validation of the snowpack model in a Montana climate. Cold Reg. Sci. Technol. 2001;33(2–3):237–246.
95. Willmott CJ, Ackleson SG, Davis RE, Feddema JJ, Klink KM, Legates DR, O'Donnell J, Rowe CM. Statistics for the evaluation and comparison of models. J. Geophys. Res. 1985;90(C5):8995.
96. Sailor DJ, Lu L. A top–down methodology for developing diurnal and seasonal anthropogenic heating profiles for urban areas. Atmos. Environ. 2004;38(17):2737–2748.
97. Middel A, Brazel A, Kaplan S, Myint S, Daytime cooling efficiency and diurnal energy balance in Phoenix, Arizona, USA. Clim. Res. 2012;54(1):21–34.
98. Qiao Z, Tian G, Xiao L. Diurnal and seasonal impacts of urbanization on the urban thermal environment: A case study of Beijing using MODIS data. ISPRS J. Photogram. Remote Sens. 2013;85:93–101.
99. Stewart ID. A systematic review and scientific critique of methodology in modern urban heat island literature. Int. J. Climatol. 2011;31(2):200–217.
100. MMD. Malaysian Meteorological Department; 2014. [Online]. Available: www.met.gov.my [Accessed: 23-Sep-2014]
101. Childs PP, Raman S. Observations and Numerical Simulations of Urban Heat Island and Sea Breeze Circulations over New York City. Pure Appl. Geophys. 2005;162(10):1955–1980.
102. Stewart I, Oke T. Local climate zones: Application to heat island studies in tropical regions. in Workshop on Urban Climatology in Tropical and Sub-Tropical Regions. 2011;1–13.
103. Elsayed I. Effects of Urbanization on the Urban Heat Island of Kuala Lumpur City: UHI As A Global Issue Kl & Urbanization Research Method Data & Findings Analaysis & Synthesis Conclusion. LAP LAMBERT Academic Publishing. 2012;1–376.
104. Ahmad S, Hashim N. Effects of Soil Moisture on Urban Heat Island Occurrences : Case of Selangor, Malaysia. Humanit. Soc. Sci. J. 2007;2(2):132–138.
105. Memon RA, Leung DYC, Liu CH. An investigation of urban heat island intensity (UHII) as an indicator of urban heating. Atmos. Res. 2009;94(3):491–500.
106. Priyadarsini R, Hien WN, Wai David CK. Microclimatic modeling of the urban thermal environment of Singapore to mitigate urban heat island. Sol. Energy. 2008;82(8):727–745.